Front. Phys. 11(1), 117101 (2016)
DOI 10.1007/s11467-015-0542-5

RESEARCH ARTICLE

Dominant ferromagnetic coupling over antiferromagnetic in Ni doped ZnO: First-principles calculations

Bakhtiar Ul Haq[1,2], Rashid Ahmed[1,*], Galila Abdellatif[5], Amiruddin Shaari[1], Faheem K. Butt[3,4], Mohammed Benali Kanoun[6], Souraya Goumri-Said[6,†]

[1] *Department of Physics, Faculty of Science, UniversitiTeknologi Malaysia, UTM Skudai, Johor81310, Malaysia*
[2] *Department of Physics, Sungkyunkwan University, Suwon 440-746, Korea*
[3] *Physik-Department ECS, Technische Universität München, James-Franck-Straße 1, 85748 Garching, Germany*
[4] *Department of Physics, The University of Lahore, 1-KM Defence Road, Lahore, Pakistan*
[5] *Department of Physics, Faculty of Science, Cairo University, Giza Egypt*
[6] *Physics Department, College of Science, AlFaisal University, P.O. Box 50927, Riyadh 11533, Saudi Arabia*
*Corresponding authors. E-mail: *rashidahmed@utm.my, †Souraya.Goumri-Said@chemistry.gatech.edu*

Received June 24, 2015; accepted November 3, 2015

The low magnetic moment (MM) in diluted magnetic semiconductors (DMS) at low impurity doping levels has triggered considerable research into condensed magnetic semiconductors (CMS).This work reports an *ab-initio* investigation of the electronic structures and magnetic properties of ZnO in a zinc-blende (ZB) structure doped with nickel ions. Ni-doped ZnO-based DMS and CMS exhibit a dominance of ferromagnetic coupling over antiferromagnetic. A robust increase in the magnetization has been observed as a function of Ni impurity levels. This material favors short-range magnetic interactions at the ground state, suggesting that the observed ferromagnetism is defined by the double exchange mechanism. The spin-polarized density of states (DOS) of Ni-doped ZnO characterizes it as half-metallic with a considerable energy gap for up-spin components and as metallic for-down spins. Half-metallic Ni:ZnO based magnetic semiconductors with high magnetization are expected to have potential applications in spintronics.

Keywords ZnO, diluted magnetic semiconductors, *ab-initio* calculations, electronic structure, magnetic properties

PACS numbers 71.15.Mb, 71.27.+a, 73.20.At, 71.20.-b

1 Introduction

Accomplishing ferromagnetic characteristics in semiconductors through doping with 3*d* elements has been practiced for several years, and has evolved into a significant field in condensed matter physics and material science [1–4]. The motivation is to extend the applications of semiconductors with coexisted magnetic features from conventional electronics to spintronic or spin-dependent electronics [1]. Advanced nano-characterization techniques allow the classification of ferromagnetic semiconductors into two distinct families, namely DMS and CMS [5–7]. In DMS, the transition metal (TM) dopants are randomly distributed in the matrix of the host semiconductor. However, the realization of functional DMS is still a major issue caused by difficulties such as the fabrication of homogeneous DMS with high magnetization [6, 7]. Moreover, the magnetization observed for lower levels of doping is many orders of magnitude smaller than the spin-only saturation magnetization [6]. This has triggered the attention of researchers towards CMS. In this class of magnetic semiconductors, high concentrations of transition metals are doped into the semiconductor matrix. Consequently, the magnetic cations have a larger density at nanoscale regions, which induces robust ferromagnetism (FM) within the matrix of the host.

The figures of merit of these materials are contingent upon the base semiconductor. The selection of suitable candidates from the numerous semiconductor species is therefore of critical importance. Research has demonstrated ZnO to be a leading host for 3d-TM dopants. ZnO is an excellent base material for magnetic semiconductors because of its wide and direct energy gap, abun-

dant availability, and environmental friendly characteristics. ZnO doped with 3d elements is predicted to have the magnetic properties demanded for an ideal magnetic semiconductor. This has stimulated a considerable interest of researchers over the past one and half decades. Earlier investigations were typically focused on W structured ZnO-based magnetic semiconductors. However, several groups are now interested in the fabrication of ZnO based magnetic semiconductors with a ZB structure, as ZB-structured ZnO with impurity elements is considered to be more appropriate for various purposes [8,9]. Moreover, in W-structured ZnO, the existence of impurity atoms induces piezoelectric effects and other unwanted built-in fields. These unwanted fields cause several effects, such as the quenching of excitonic effects [10], that reduce the efficiency of ZnO in technological applications. However, ZB-structured ZnO is free from such unwanted fields, and is expected to have more applications than W-structured ZnO.

The literature shows a number of theoretical and experimental studies where ZB-ZnO was efficiently doped with impurity atoms for spintronic and other productive applications. For instance, Limaye *et al.* [8] doped ZB-ZnO with Mn to inject MM to obtain DMS. By adapting the chemical route approach, they successfully fabricated ZnO on ZnS nano-particles. Zhang *et al.* [11] have investigated the electronic structure and magnetic properties of Co-doped ZnO in the ZB phase. They have reported antiferromagnetism (AFM) at the ground state, and FM at the meta-stable state. Mamouni *et al.* [12] have studied the electronic and magnetic properties of ZB V:ZnO using the Korringa–Kohn–Rostoker method based on the first principles approach. They demonstrated the half-metallic nature of V:ZnO with stable FM ordering. Xu *et al.* [13] have used the FP-L (APW+lo) method to investigate the effect of C impurities in ZB-ZnO. Their results showed the half-metallic nature of ZB C:ZnO with a MM of magnitude 2.0 μ_B. They reported the low formation energy of C:ZnO in the ZB geometry, and consequently stable C:ZnO in the cubic phase. Li *et al.* [14] have investigated the effect of Cu impurity atoms on the electronic and magnetic properties of ZB ZnO. Their investigations showed that Cu impurities can induce MMs of magnitude 1.0 μ_B in the stable FM ground state.

Among TM elements, Ni^{2+} is considered as one of the most appropriate dopants for ZnO due to its nearly similar atomic radius and oxidation state to that of Zn^{2+} [15]. Therefore, Ni-doped ZnO has been the subject of several studies, however, theoretical and experimental disagreement remains regarding the nature of the magnetization. Wakano *et al.* experimentally investigated the magnetic properties of Ni:ZnO containing 25% of Ni content fabricated utilizing the pulsed laser deposition (PLD) method [16]. They observed FM interactions in Ni:ZnO with a T_c of 2 K. Their study showed that FM was transformed to PM in the temperature range 30 K to 300 K. However, room temperature FM was observed in ZnO in the presence of Ni dopants in the experimental studies of Jung *et al.* [17] and Cui [18]. Similarly, Venkatesan *et al.* [19] have reported room temperature FM in Ni:ZnO thin films containing 5% Ni. In addition, there have been several studies reporting intrinsic room temperature FM in Ni-substituted ZnO [20–24]. Li *et al.* [25] have claimed an observation of FM in the Ni:ZnO system, that was induced by Ni clusters or secondary phases. Recently, the properties and clustering behavior of Ni pairs was also investigated theoretically [26]. In line with the predictions of Li *et al.* [25], they have reported the clustering tendency of Ni ions in the Ni:ZnO system and claimed the Ni clusters were responsible for the observed FM. The reports of the intrinsic paramagnetic (PM) nature of Ni-doped ZnO systems [27] are contradictory, and results in difficulties for their application in spintronics. The PM nature was further confirmed by Yin *et al.* [28], who fabricated Ni:ZnO containing 14% Ni, which demonstrated PM rather than FM. Pie *et al.* [29] studied the magnetic interactions in Ni-doped ZnO using GGA and GGA+U (U is Hubbard parameter) schemes and have predicted FM ordering. Similarly, some efforts to observe ferromagnetism with Ni doping were carried out experimentally and the solubility of Ni was reported to be 25% [11, 16]. Furthermore, ZnO films doped with Ni (x=0.03 to 0.25) exhibit ferromagnetic behavior at 350 K. However, Straumal *et al.* have recently shown the possibility of manipulating the grain size to increase the Ni solubility in ZnO [30].

In the present study, Ni-doped ZB-structured ZnO-based DMS and CMS has been explored over a range of Ni-dopant concentrations: 6.25%, 12.5%, 18.75%, 25%, 50%, and 75%. We have employed first principles calculations based on the FP-L (APW+lo) method with the generalized gradient approximation: GGA and GGA+U functionals methodology to investigate the electronic and magnetic properties of Ni-doped ZnO.

2 Computational details

Our calculations were performed using the first principles full-potential linear augmented plane wave plus local orbitals method within DFT, as implemented in WIEN2k code [31]. The exchange and correlations were treated within the Perdew–Burke–Ernzerhof generalized gradient approximation [32], including the Hubbard cor-

rection, known as the GGA+U method. In the FP-L (APW+lo) method, the unit cell is divided into two regions, namely the non-overlapping atomic spheres or core region, and interstitial regions, with different basis sets used in both the regions to expand the Kohn–Sham wave functions, charge density, and potential. Inside the core region, a linear combination of radial functions times spherical harmonics is used, while in the interstitial region a plane wave expansion is used [32]. The muffin-tin radii (R_{MT}) values for Zn and Ni are selected as 1.78 a.u., with a value of 1.5 a.u. for O atoms. A dense k-mesh with 72 k-points is employed in the special irreducible Brillion zone (BZ). The energy cutoff is taken as $k_{\max} = 8.0/R_{\mathrm{MT}}$. To overcome the band gap deficiency of the DFT, an additional Hubbard parameter with u_{eff} = 7.1 eV [33] is employed.

3 Results and discussion

In magnetic semiconductors, one of the factors that most strongly affects their properties is the substitution of impurity atoms onto the proper dopant sites. To find appropriate dopant sites for the impurity atoms, the total energies have been calculated corresponding to various doping positions (Fig. 1). Table1 presents the details of total energies corresponding to different doping positions. In order to investigate the stability of short/long magnetic interactions in the ground state, two different spatial arrangements referred to as C1 and C2 based on the Ni substitution sites are investigated. In the C1 configuration, the Ni dopants are placed at the minimum distance to the nearest Ni neighbor. The two

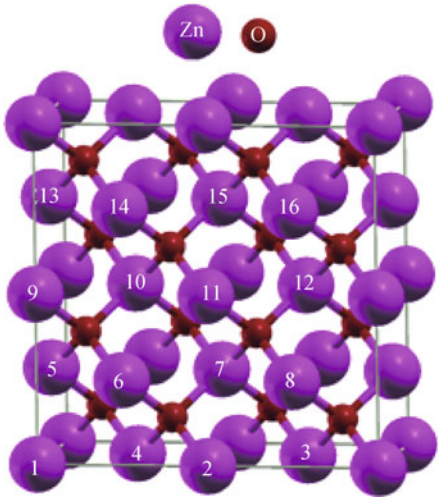

Fig. 1 Schematic structures of Ni:ZnO ZB geometry. The numbered spheres show the Ni/Zn substitutional sites; the purple colored large spheres and the red colored small spheres represent zinc and oxygen atoms, respectively.

Table 1 Symmetry breaking of Ni:ZnO in ZB geometry for different Ni substitutional sites and their corresponding energies.

Composition	Zn/Ni position	Symmetry	Energy/Formula Unit (R_y)
$Zn_{15}Ni_1O_{16}$	10	P	–3708.3712
	10	P-42m	–3708.3716
$Zn_{14}Ni_2O_{16}$	10,12	P	–3673.9105
	10,12	P-42m	–3673.9524
	10,15	Cmm2	–3673.9639
$Zn_{13}Ni_3O_{16}$	7,10,12	P	–3673.9687
	7,10,12	P2	–3639.5433
	7,10,15	P2	–3639.5432
	10,11,12	P222	–3639.5438
$Zn_{12}Ni_4O_{16}$	2,7,10,12	P	–3605.1190
	2,7,10,12	P2	–3605.1228
	6,7,8,12	P1	–3605.1248
	6,7,10,12	P1	–3605.1248
	4,7,10,16	P2	–3605.1228
	6,7,14,15	P2221	–3605.1154
	6,11,14,16	Cm	–3605.1245

neighboring Ni atoms are separated by a single O-anion, i.e., Ni-O-Ni. In the latter case, the Ni dopants are separated by two O-anions and one Zn-cation, i.e., Ni-O-Zn-O-Ni, which results in a comparatively larger distance. The total energies for C1 and C2 are calculated as –3673.9562 Ry and –3673.9559 Ry respectively. The comparatively lower energy in C1 suggesting that Ni:ZnO-based magnetic semiconductors favor short-range Ni-Ni magnetic coupling and have a tendency to cluster together.

To investigate the structural properties of Ni:ZnO, the lattice parameters were calculated by fitting the unit cell volume against the total energies using Murnaghan's equation of state [34]. The lattice parameters results are depicted in Table 2. The lattice parameters of ZnO in the presence of Ni are nearly equivalent to that of pure ZnO [35]. The variation in lattice parameters was insignificant up to 28% Ni content. Yin *et al.* [28] have experimentally demonstrated an insignificant effect on the lattice parameters of W-structured Ni:ZnO until the Ni concentration reaches 20%, beyond which the lattice parameter decreases almost linearly as a function of Ni content because the ionic radii of Ni (0.69 Å) is smaller than Zn (0.74 Å). Our results for the variation of lattice parameters of ZnO in the presence of Ni contents are in good agreement with the experimental findings [21, 23]. The total variation of the lattice parameters of ZnO when doped with concentrations between 6.25% to 75% Ni was found to be 0.9 Å.

To investigate the electronic properties of the Ni:ZnO system, the spin-polarized total DOS and partial DOS were determined. The DOS profile of the Ni:ZnO system

Table 2 Calculated lattice parameter a of Ni:ZnO in ZB structure.

Ni:ZnO	6.25%	12.5%	18.75%	25%	50%	75%
a (Å)	4.61	4.61	4.61	4.60	4.54	4.50

reflects significant changes as compared to our previously calculated DOS for pure ZB-ZnO [34–38]. Since the spin-polarized DOS for Ni:ZnO exhibits similar resemblance for all dopant contents, an optimal picture of the total and partial DOS will be displayed for $Zn_{0.875}Ni_{0.125}O$ only. Figure 2 depicts the spin-polarized total DOS of $Zn_{0.875}Ni_{0.125}O$ at the level of the GGA+U approximation. For the GGA method, we observed that the Fermi level appears in the conduction band (CB) for the spin-up channels, however, by applying an additional U-parameter to GGA, a gap between the valence and conduction bands was observed. In the case of down-spin electrons, a broad impurity band appears in the Fermi level that leads to metallic Ni:ZnO. The simultaneous semiconducting and metallic nature of Ni:ZnO for up and down spin channels respectively, introduces Ni:ZnO to a class of materials known as half-metallic. This characteristic of Ni:ZnO endorses its application as a filter for spin-polarized currents, as well as in other spin-dependent electronic devices.

In the spin-polarized partial DOS of Ni:ZnO (Fig. 3), the structures shown in the deep valence band (VB) (–6 to –4.8 eV) mostly originate from Zn-3d states; in the energy range from –4.8 eV to –2.3 eV, the states were contributed by the Zn-3d and O-2p states together with a weak effect on the Ni-3d states. In the case of up-spin DOS the structures in the energy range from –2 to –1 eV were due to the Ni-3d states together with O-2p states, where the 5-fold degeneracy of the Ni-3d band was transformed to sub $e_g(dx^2-y^2$ and $dz^2)$ and $t_{2g}(dxy, dzx, dyz)$ bands due to the tetragonal O^{2-} environment. For the down-spin case, the Ni-3d states in the vicinity of the Fermi level were again split into e_g and t_{2g} by the crystal

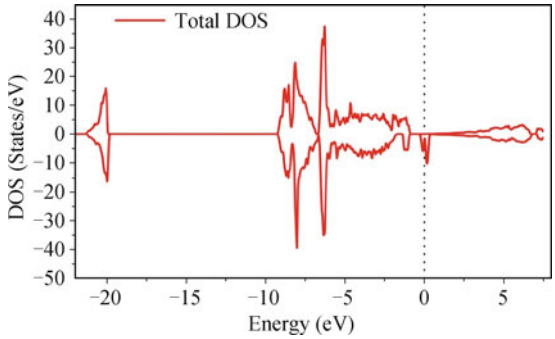

Fig. 2 Calculated spin polarized total density of states of Ni:ZnO for 12.5% Ni contents. The states in positive energies represent the majority spin carriers and the states in negative energies resemble the minority spin carriers.

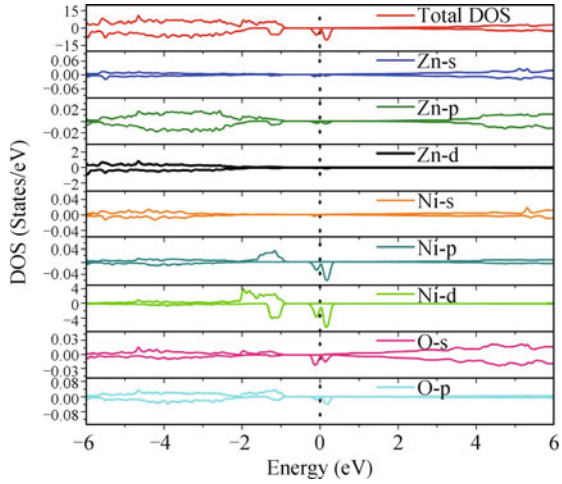

Fig. 3 Spin-polarized total and partial DOS of Ni: ZB phases at 12.5% of Ni contents. The dotted line reveals the Fermi level; the states in positive energies represent the majority spin carriers and the states in negative energies resemble the minority spin carriers.

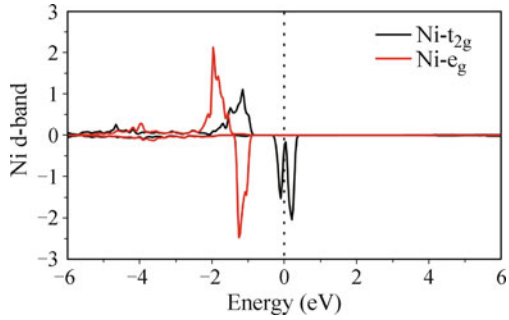

Fig. 4 Splitting of Ni d-band into e_g and t_{2g} states due to the Coulomb potential produced by O atoms.

field effect. Ni d-band splitting is schematically shown in Fig. 4. It is observed that the e_g and t_{2g} band's energies strongly depend on the geometry of the crystal. In the ZB phase, the O-ions induced a tetrahedral Coulomb environment, where the t_{2g} states reside closer to O^{2-} and thus are higher in energy compared to the e_g states. The structures at the CB minima for the up-spin DOS were due to Zn-4s, while for the down-spin DOS the structures at the CB minima were due to Ni-t_{2g} states.

We further investigated the DOS defined by p-electrons of O atoms that were directly associated with the Ni atoms, labeled as O1, and of those placed away from Ni, labeled as O2 (Fig. 5). Our analysis shows higher binding energies of O1-p electrons compared to O2-p electrons. The higher binding energies of O1-p electrons is possibly caused by the electrostatic coulomb potential due to the nearest Ni atoms, from where they experience a higher coulomb repulsion compared to O2 electrons.

An investigation of the magnetic properties of Ni:ZnO was performed to explore the nature of its magnetiza-

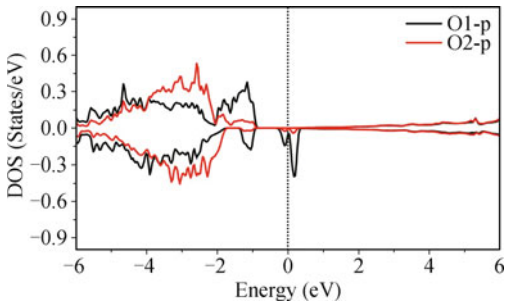

Fig. 5 Partial DOS of *p*-electrons associated to O1 and O2 atoms.

tion. For this purpose, the total energies per formula unit for ferromagnetic and antiferromagnetic spin components were measured. In the ferromagnetic mode, the spin of the impurity atoms was fixed on the same axis, while in the antiferromagnetic mode the spin of impurity atoms is aligned in opposite directions, such that they cancel out the effect of each other. The dominant FM/AFM spin mode was characterized by difference in the energies ($\Delta E = E_{\mathrm{AFM}} - E_{\mathrm{FM}}$). The calculated energies in the FM and AFM states are summarized in Table 3. It is evident that Ni:ZnO exhibited FM behavior for the entire range of Ni contents (Table 3). At lower Ni contents or DMS, FM is considered to be caused by intrinsic Ni dopants. In the present study, the FM observed for higher magnetic contents or CMS was caused by the combined effect of the ferromagnetic Ni clusters embedded in the ZnO matrix. The FM character of Ni:ZnO for various concentrations has also been reported by Fu *et al.* [38]. Our calculations for the MM per formula unit of Ni:ZnO were summarized in Table 4. The occurrence of FM in the non-magnetic ZnO suggests that Ni atoms are the main contributor to the observed magnetization. The calculated MM in Ni:ZnO is strongly dependent on the Ni concentration. The MM increases almost linearly with the Ni content.

To complete the magnetic description, we have plotted in Fig. 6 the spin and charge densities iso-surfaces in 3D for a Ni concentration of 25% in ZnO. We can observe a strong localization at the Ni sites, whereas the Zn and

Table 3 Summary of the calculated total energies (in R_y) of ZB Ni:ZnO in FM and AFM ground-state magnetic ordering.

Ni:ZnO	E_{FM}	E_{AFM}	Coupling
$Zn_{15}Ni_1O_{16}$	–3708.3713	–3708.3681	FM
Zn_{14} Ni_2O_{16}	–3673.9569	–3673.9566	FM
Zn_{13} Ni_3O_{16}	–3639.5438	–3639.5285	FM
Zn_{12} Ni_4O_{16}	–3605.1190	–3605.1120	FM
Zn_8 Ni_8O_{16}	–3467.4455	–3467.4119	FM
Zn_4 $Ni_{12}O_{16}$	–3329.7758	–3329.7677	FM

Table 4 Calculated total MM (in μ_B) per formula unit in Ni:ZnO.

MM	6.25%	12.5%	18.75%	25%	50%	75%
Ni:ZnO	0.13	0.25	0.33	0.50	1	1.49

O atoms show much less polarization in agreement with PDOS and the results reported in Table 2. From the charge density iso-surface, we can see that the additional charge carriers due to Ni doping in ZnO promote ferromagnetism in ZnO [39, 40]. In fact, one can observe a significant amount of charge transferred from Ni to the O-atoms, reflecting the possibility of an ionic bonding nature [41].

Several models have been presented to explain the origin of FM in magnetic semiconductors, such as bound magnetic polarons, double exchange and super exchange interactions, the phenomenological Zener/Ruderman–Kittel–Kasuya–Yosida (RKKY) model [42], and spin-split donor impurity models. In the present work, RKKY interactions are believed to be one of the reasons why Ni:ZnO favors FM if the impurity atoms are located in the short range positions. Moreover, the double exchange mechanism, which explains the FM if the impurity bands appear in the band gap, is also believed to determine the FM.

4 Conclusions

In the present study, DFT calculations using the FP-L (APW+*lo*) basis set have been used to explore the

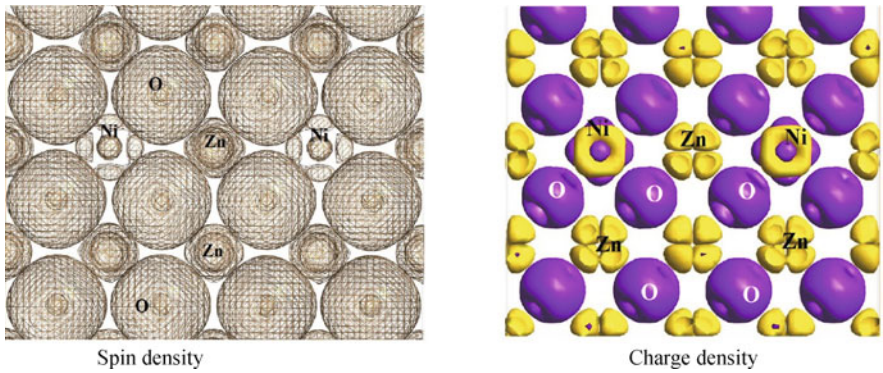

Fig. 6 Spin density and charge density iso-surfaces of ZnO:Ni at Ni composition 25%.

physical properties of Ni-doped ZB-structured ZnO-based DMS and CMS. The lower magnetic moment in DMSs at the cost of lower magnetic ions has shown a robust increase in case of CMS. The higher magnetization in the Ni:ZnO based CMS is possibly caused by the combined effects of the nanoscale clusters with large Ni-ion densities in the matrix of the ZnO. The FM observed in Ni:ZnO remains dominant over AFM for all the doping contents investigated. The DOS profile of Ni:ZnO shows a half-metallic nature appropriate for spin dependent electronic applications.

Acknowledgements B. U. H. and R. A. would like to acknowledge the financial support of the Ministry of Education (MOE)/Universiti Teknologi Malaysia (UTM) through Grant Nos. Q.J130000.2526.02H89, R.J130000.7826.4F113, and Q.J130000.2526.04H14.

References

1. Y. Ohno, D. Young, B. Beschoten, F. Matsukura, H. Ohno, and D. Awschalom, *Nature* 402(6763), 790 (1999)
2. T. Dietl, H. Ohno, F. Matsukura, J. Cibert, and D. Ferrand, Zener model description of ferromagnetism in zinc-blende magnetic semiconductors, *Science* 287(5455), 1019 (2000)
3. T. Fukumura, Z. Jin, M. Kawasaki, T. Shono, T. Hasegawa, S. Koshihara, and H. Koinuma, Magnetic properties of Mn-doped ZnO, *Appl. Phys. Lett.* 78(7), 958 (2001)
4. T. Fukumura, Z. Jin, A. Ohtomo, H. Koinuma, and M. Kawasaki, An oxide-diluted magnetic semiconductor: Mn-doped ZnO, *Appl. Phys. Lett.* 75(21), 3366 (1999)
5. A. Bonanni and T. Dietl, A story of high-temperature ferromagnetism in semiconductors, *Chem. Soc. Rev.* 39(2), 528 (2010)
6. I. Bilecka, L. Luo, I. Djerdj, M. D. Rossell, M. Jagodic, Z. Jaglicic, Y. Masubuchi, S. Kikkawa, and M. Niederberger, Microwave-assisted nonaqueous sol–gel chemistry for highly concentrated ZnO-based magnetic semiconductor nanocrystals, *J. Phys. Chem. C* 115(5), 1484 (2011)
7. F. Filippone, G. Mattioli, P. Alippi, and A. A. Bonapasta, Clusters and magnetic anchoring points in (Ga,Fe)N condensed magnetic semiconductors, *Phys. Rev. Lett.* 107(19), 196401 (2011)
8. M. V. Limaye, S. B. Singh, S. K. Date, R. Gholap, and S. K. Kulkarni, Epitaxially grown zinc-blende structured Mn doped ZnO nanoshell on ZnS nanoparticles, *Mater. Res. Bull.* 44(2), 339 (2009)
9. A. Ashrafi and C. Jagadish, Review of zincblende ZnO: Stability of metastable ZnO phases, *J. Appl. Phys.* 102(7), 071101 (2007)
10. G. Lee, T. Kawazoe, and M. Ohtsu, Room temperature near-field photoluminescence of zinc-blend and wurtzite ZnO structures, *Appl. Surf. Sci.* 239(3), 394 (2005)
11. J. Zhang, K. Yao, Z. Liu, and G. Gao, First principles calculations of Co-doped zinc-blende ZnO magnetic semiconductor, *Physica B* 405(6), 1447 (2010)
12. N. Mamouni, M. Belaiche, A. Benyoussef, A. El Kenz, H. Ez-Zahraouy, M. Loulidi, E. Saidi, and E. Hlil, Electronic and magnetic structures of V-doped zinc blende $Zn_{1-x}V_xN_yO_{1-y}$ and $Zn_{1-x}V_xP_yO_{1-y}$, *Chin. Phys. B* 20(8), 087504 (2011)
13. C. C. Xu, L. Jiang, N. Leng, and P. J. Liu, Selective triggering of phase change in dielectrics by femtosecond pulse trains based on electron dynamics control, *Chin. Phys. B* 22(4), 047507 (2013)
14. X. Li, J. Zhang, B. Xu, and K. Yao, Half-metallic ferromagnetism in Cu-doped zinc-blende ZnO from first principles study, *J. Magn. Magn. Mater.* 324(4), 584 (2012)
15. B. U. Haq, R. Ahmed, A. Afaq, A. Shaari, and M. Zarshenas, Structural and electronic properties of ni-doped ZnO in zinc-blende phase: A DFT investigations, in: International Conference on Fundamental and Applied Sciences 2012 (ICFAS2012), AIP Publishing, 2012
16. T. Wakano, N. Fujimura, Y. Morinaga, N. Abe, A. Ashida, and T. Ito, Magnetic and magneto-transport properties of ZnO:Ni films, *Physica E* 10(1), 260 (2001)
17. S. W. Jung, W. I. Park, G. C. Yi, and M. Kim, Fabrication and controlled magnetic properties of Ni/ZnO nanorod heterostructures, *Adv. Mater.* 15(16), 1358 (2003)
18. J. Cui and U. Gibson, Electrodeposition and room temperature ferromagnetic anisotropy of Co and Ni-doped ZnO nanowire arrays, *Appl. Phys. Lett.* 87(13), 133108 (2005)
19. M. Venkatesan, C. Fitzgerald, J. Lunney, and J. Coey, Anisotropic ferromagnetism in substituted zinc oxide, *Phys. Rev. Lett.* 93(17), 177206 (2004)
20. B. Li, X. Xiu, R. Zhang, Z. Tao, L. Chen, Z. Xie, Y. Zheng, and Z. , Study of structure and magnetic properties of Ni-doped ZnO-based DMSs, *Mater. Sci. Semicond. Process.* 9(1), 141 (2006)
21. D. L. Hou, R. B. Zhao, Y. Y. Wei, C. M. Zhen, C. F. Pan, and G. D. Tang, Room temperature ferromagnetism in Ni-doped ZnO films, *Curr. Appl. Phys.* 10(1), 124 (2010)
22. B. Pandey, S. Ghosh, P. Srivastava, D. Avasthi, D. Kabiraj, and J. Pivin, Synthesis and characterization of Ni-doped ZnO: A transparent magnetic semiconductor, *J. Magn. Magn. Mater.* 320(24), 3347 (2008)
23. C. Cong, J. Hong, Q. Liu, L. Liao, and K. Zhang, Synthesis, structure and ferromagnetic properties of Ni-doped ZnO nanoparticles, *Solid State Commun.* 138(10), 511 (2006)
24. G. Pei, C. Xia, S. Cao, J. Zhang, F. Wu, and J. Xu, Synthesis and magnetic properties of Ni-doped zinc oxide powders, *J. Magn. Magn. Mater.* 302(2), 340 (2006)
25. T. Li, H. Qiu, P. Wu, M. Wang, and R. Ma, Characteristics of Ni-doped ZnO:Al films grown on glass by direct current magnetron co-sputtering, *Thin Solid Films* 515(7), 3905 (2007)

26. G. Gu, G. Xiang, J. Luo, H. Ren, M. Lan, D. He, and X. Zhang, Magnetism in transition-metal-doped ZnO: A first-principles study, *J. Appl. Phys.* 112(2), 023913 (2012)
27. Z. Jin, T. Fukumura, M. Kawasaki, K. Ando, H. Saito, T. Sekiguchi, Y. Yoo, M. Murakami, Y. Matsumoto, T. Hasegawa, and H. Koinuma, High throughput fabrication of transition-metal-doped epitaxial ZnO thin films: A series of oxide-diluted magnetic semiconductors and their properties, *Appl. Phys. Lett.* 78(24), 3824 (2001)
28. Z. Yin, N. Chen, F. Yang, S. Song, C. Chai, J. Zhong, H. Qian, and K. Ibrahim, Structural, magnetic properties and photoemission study of Ni-doped ZnO, *Solid State Commun.* 135(7), 430 (2005)
29. G. Pei, C. Xia, B. Wu, T. Wang, L. Zhang, Y. Dong, and J. Xu, Studies of magnetic interactions in Ni-doped ZnO from first-principles calculations, *Comput. Mater. Sci.* 43(3), 489 (2008)
30. B. B. Straumal, A. A. Myatiev, P. B. Straumal, A. A. Mazilkin, S. G. Protasova, E. Goering, and B. Baretzky, Grain boundary layers in nanocrystalline ferromagnetic zinc oxide, *JETP Lett.* 92(6), 396 (2010)
31. P. Blaha, K. Schwarz, G. Madsen, D. Kvasnicka, and J. Luitz, An augmented plane wave plus local orbitals program for calculating crystal properties, Vienna University of Technology, Austria, 2001
32. J. P. Perdew, K. Burke, and M. Ernzerhof, Generalized Gradient Approximation Made Simple, *Phys. Rev. Lett.* 77(18), 3865 (1996)
33. V. I. Anisimov, J. Zaanen, and O. K. Andersen, Band theory and Mott insulators: Hubbard U instead of Stoner I, *Phys. Rev. B* 44(3), 943 (1991)
34. F. Murnaghan, The compressibility of media under extreme pressures, *Proc. Natl. Acad. Sci. USA* 30(9), 244 (1944)
35. B. Ul Haq, R. Ahmed, S. Goumri-Said, A. Shaari, and A. Afaq, Electronic structure engineering of ZnO with the modified Becke–Johnson exchange versus the classical correlation potential approaches, *Phase Transitions* 86 (12), 1167 (2013)
36. B. Ul Haq, R. Ahmed, R. Khenata, M. Ahmed, and R. Hussain, A first-principles comparative study of exchange and correlation potentials for ZnO, *Mater. Sci. Semicond. Process.* 16 (4), 1169(2013)
37. B. Ul Haq, A. Afaq, R. Ahmed, and S. Naseem, A Comprehensive DFT study of zinc oxide in different phases, *Int. J. Mod. Phys. C* 23(06), 1250043 (2012)
38. J. Fu, B. Wu, H. Liu, C. Zhang, M. Lin, and L. Chen, Structural and magnetic ordering behaviour of (Co, Ni, and Al) doped ZnO diluted magnetic semiconductor, in: 2010 Symposium on Photonics and Optoelectronic (SOPO), IEEE, 2010
39. B. Ul Haq, R. Ahmed, A. Shaari, and S. Goumri-Said, GGA+U investigations of impurity d-electrons effects on the electronic and magnetic properties of ZnO, *J. Magn. Magn. Mater.* 362, 104 (2014)
40. B. Ul Haq, R. Ahmed, and S. Goumri-Said, Tailoring ferromagnetism in chromium-doped zinc oxide, *Mater. Res. Exp.* 1(1), 016108 (2014)
41. S. Goumri-Said, M. B. Kanoun, A. Manchon, and U. Schwingenschlögl, Spin-polarization reversal at the interface between benzene and Fe(100), *J. Appl. Phys.* 113(1), 013905 (2013)
42. M. A. Ruderman and C. Kittel, Indirect exchange coupling of nuclear magnetic moments by conduction electrons, *Phys. Rev.* 96(1), 99 (1954)